Pflugers Arch - Eur J Physiol
DOI 10.1007/s00424-016-1928-0

The inhibition of voltage-gated H^+ channel (HVCN1) induces acidification of leukemic Jurkat T cells promoting cell death by apoptosis

Agustín Asuaje[1] · Paola Smaldini[1] · Pedro Martín[1] · Nicolás Enrique[1] · Alejandro Orlowski[2] · Ernesto A. Aiello[2] · Carlos Gonzalez León[3] · Guillermo Docena[1] · Verónica Milesi[1]

Received: 2 September 2016 / Revised: 5 December 2016 / Accepted: 6 December 2016

Abstract Cellular energetic deregulation is widely known to produce an overproduction of acidic species in cancer cells. This acid overload must be counterbalanced with a high rate of H^+ extrusion to maintain cell viability. In this sense, many H^+ transporters have been reported to be crucial for cell survival and proposed as antineoplastic target. By the way, voltage-gated proton channels (Hv1) mediate highly selective H^+ outward currents, capable to compensate acid burden in brief periods of time. This structure is canonically described acting as NADPH oxidase counterbalance in reactive oxygen species production. In this work, we show, for the first time in a oncohematologic cell line, that inhibition of Hv1 channels by Zn^{2+} and the more selective blocker 2-(6-chloro-1H-benzimidazol-2-yl)guanidine (ClGBI) progressively decreases intracellular pH in resting conditions. This acidification is evident minutes after blockade and progresses under prolonged exposure (2, 17, and 48 h), and we firstly demonstrate that this is followed by cell death through apoptosis (annexin V binding). Altogether, these results contribute strong evidence that this channel might be a new therapeutic target in cancer.

Keywords HVCN1 · Voltage-gated proton channel · Intracellular pH · Apoptosis · Leukemia · Cancer

Introduction

Voltage-gated H^+ channels (Hv1), encoded by the *hvcn1* gene, mediate highly selective H^+ outward currents [42], avoiding cell acidification and depolarization. This relevant homeostatic function of Hv1 channels is essential for a variety of immune cells such as neutrophils [33, 46, 57], eosinophils [9, 21, 39], basophiles, B lymphocytes [6] as well as spermatozoa [34], osteoclasts [44], and myocardial fibroblasts [7]. The intracellular pH (pH_i), which typically ranges in a narrow window (7.2–7.4), is finely controlled for cell survival since the vast majority of cell machinery has a well-defined pH for optimal activity (i.e., enzyme activity). Indeed, intracellular acidification is an early key event leading to cell death by different apoptotic stimuli [31, 36, 37]. Particularly, in cancer cells, it has been widely demonstrated that, regardless of the amount of oxygen available, a metabolic deregulation promotes the use of the less efficient glycolytic pathway increasing acidic species concentration [29, 56]. In the absence of compensatory mechanisms, tumor cell survival would be compromised. Thus, cell structures capable of reducing the acid load in tumor cells give them an advantage to escape from the acidification-related cell death. Hv1 channels are excellent candidates that can contribute to this process. The activity of Hv1 channels allows a quick compensation of acidic cell

Electronic supplementary material The online version of this article (doi:10.1007/s00424-016-1928-0) contains supplementary material, which is available to authorized users.

✉ Pedro Martín
pedromartinv@gmail.com

[1] Instituto de Estudios Inmunológicos y Fisiopatológicos (IIFP, CONICET—Universidad Nacional de la Plata), Fac. de Ciencias Exactas, Universidad Nacional de La Plata, 47 y 115, 1900 La Plata, Argentina

[2] Centro de Investigaciones Cardiovasculares (CIC, CONICET—Universidad Nacional de la Plata), Fac. de Ciencias Médicas, Universidad Nacional de La Plata, 60 y 120, 1900 La Plata, Argentina

[3] Centro Interdisciplinario de Neurociencia de Valparaíso, Facultad de Ciencias, Universidad de Valparaíso, Chile, Pasaje Harrington 287, Playa Ancha, Valparaíso, Chile

Published online: 24 December 2016

production without metabolic energy cost. It has been reported that Hv1 can restore cytoplasmic pH after heavy acid loads with a high efficacy (few seconds) in different cell types [5, 8, 14, 27, 40, 41, 55, 60]. Moreover, in solid tumors such as colorectal and breast cancer cells, Hv1 inhibition with Zn^{2+} produces acidification, a decrease in cell proliferation, and migration. In both tumors, Wang et al. have proved a clinicopathological correlation where high Hv1 expression is associated with shorter overall and recurrence-free survival of patients [63, 64].

In Jurkat T cells originated from a human acute leukemia, Gottlieb et al. demonstrated that intracellular acidification is an early event of the apoptotic process when these cells receive pro-apoptotic stimuli such as anti-Fas, cycloheximide, or UV light [22]. Although they demonstrated that this step is necessary for the death process to continue, it is poorly understood which mechanisms are responsible for the pH drop.

Since Hv1 channels are functionally expressed in Jurkat T cells [53], we have hypothesized that Hv1 channel activity could preclude cellular acidification representing an antiapoptotic advantageous mechanism in oncohematological cells to prolong its survival. On the contrary, cells subject to intracellular acidification by Hv1 blocking are highly prone to cell death by apoptosis. Potentially, Hv1 inhibition could be an additional ion channel target to induce leukemic cell death together with other ion channels already proposed [1] as well as other structures that induce H^+ efflux which were considered as auspicious targets in experimental oncology [58]: the Na^+/H^+ exchanger (NHE1), the monocarboxylic acid transporter (MCT4), and the V-ATPase.

In this study, we proved that the sole inhibition of Hv1 channels with Zn^{2+} or the more selective Hv1 inhibitor, the guanidine derivative 2-(6-chloro-1H-benzimidazol-2-yl)guanidine (ClGBI) [24], induced a progressive intracellular acidification. And, for the first time, we show that Hv1 blockade not only reduces proliferation but also induces apoptosis cell death.

Methodology

Cell culture

Jurkat T cells were grown in DMEM high-glucose (25 mM) medium supplemented with 10% (*v*/*v*) heat-inactivated fetal bovine serum (Internegocios), in 5% CO_2/95% humidified air at 37 °C at an average density of 10^6 cells/ml.

Patch clamp experiments

The cells were observed with a mechanically stabilized, inverted microscope (Telaval 3, Carl Zeiss, Jena) equipped with a 40× objective lens. The standard tight-seal whole-cell configuration of the patch clamp technique was used to record macroscopic whole-cell currents [23]. Pipettes were drawn from capillary glass (PG52165-4, WPI, Boca Raton, FL, USA) on a two-stage vertical micropipette puller (PP-83, Narishige, Tokyo, Japan), and pipette resistances were 2–4 MΩ measured in extracellular saline solution (ESS). Ionic currents were measured with an appropriate amplifier (Axopatch 200A, Axon Instruments, Foster City, CA, USA). Whole-cell currents were filtered at 2 kHz, digitized (Digidata 1440, Molecular Devices, LLC, Orleans Drive, Sunnyvale, CA, USA) at a sample frequency of 10 kHz, and stored on a computer hard disk for later analysis. Total cell membrane capacitance was estimated by integrating the capacitive current transient elicited by the application of 10 mV hyperpolarizing step pulse from a holding potential of −60 mV. The estimated membrane capacitance of Jurkat T cells was 8.5 ± 2.8 pF (n = 18). Series resistance ranged from 10 to 15 MΩ. All the experiments where performed using an agar salt bridge.

Application of test solutions was performed through a multibarreled pipette positioned close to the cell investigated. After each experiment on a single cell, the experimental chamber was replaced by another one containing a new sample of cells. All experiments were performed at room temperature (~22 °C).

The ESS used for recording H^+ currents contained the following (in mM): 100 4-(2-hydroxyethyl)piperazine-1-ethanesulfonic acid (HEPES), 2 $MgCl_2 \cdot 6H_2O$, 90 *N*-methyl-D-glucamine (NMDG), 1 ethyleneglycol-bis(b-aminoethylether)-*N*,*N*,*N*,*N*′-tetraacetic acid (EGTA), and pH adjusted to 7.8 with HCl. The composition of the intracellular pipette solution (IPS) contained the following (in mM): 100 MES, 2 $MgCl_2 \cdot 6H_2O$, 90 NMDG, 1 EGTA, and pH adjusted to 6.3 with HCl.

For Hv1 blockade experiments, ClGBI solutions were made adding appropriate amounts of a 100 mM stock in dimethyl sulfoxide (DMSO) to ESS on the day of the experiment; corresponding controls contained 0.8% DMSO in ESS.

Fluorometric pH_i determination

Jurkat T cells were incubated with 10 μg/ml of 2′,7′-bis-(2-carboxyethyl)-5-(6)-carboxyfluorescein acetoxymethyl ester (BCECF-AM) for 20 min at 37 °C. Then, the dye-loaded cells were separated by centrifugation (700×*g*, 2 min), suspended in HEPES-buffered solution, re-incubated for 15 min in dye-free solution to complete the hydrolysis, washed, and suspended at a density of 2 × 10^7 cells/ml. Aliquots of 50 μl of this suspension were diluted in 2 ml of HEPES-buffered solution for the measurement of the pH_i changes in the stirred and thermostatted cuvette of a spectrofluorometer Aminco-Bowman series II (Silver Spring, MD, USA). The suspension of cells loaded with BCECF was excited at 503 and 440 nm,

and the emitted fluorescence was collected at 535 nm. Cells were exposed to propionic acid to acidify the intracellular milieu; the recovery rate was measured in the presence of Zn^{+2} (1 mM nominal) or Hv1 blocker, ClGBI (200 μM). Initial velocity of pH_i recovery for Jurkat T cells subjected to an acid load was calculated by fitting a linear regression of the first minute of the pH_i recovery after maximum acidosis. pH_i was calculated in each preparation calibrating with a high potassium-nigericin solution (135 mM KCl replaced the same concentration of NaCl in the HEPES solution, with 10 μM nigericin, titrated with KOH to pH 7.8). Small volumes of 0.1 M HCl were added to decrease pH stepwise to 6.5. The relationship between the ratios of fluorescence 503/440 nm and the pH value obtained in each step was linear.

HEPES solution contained the following (mM): 133 NaCl, 5 KCl, 1.2 $MgSO_4$, 0.8 $MgCl_2$, 10 glucose, 1.35 $CaCl_2$, and 10 HEPES, pH adjusted to 7.4 with NaOH. In sodium-free experiments, NaCl was replaced by choline chloride in the same concentration.

In vitro exposure of Jurkat T cell line to Hv1 channel blockers for flow cytometry determinations

Cells were incubated in 96-well plates (200 μl/well) at a starting concentration of 0.5×10^6 cells/ml and cultured in the conditions abovementioned (see "Cell culture" section) in normal Na^+ concentration. Cells were exposed for 2 and 17 h with Zn^{2+} (1 mM nominal) prior to the measurements. Due to medium complexity (mainly serum), it was hardly possible to calculate free Zn^{2+} concentration, and as it is known that this value is far below nominal [45], 1 mM was chosen to ensure a significant channel blockade. Independently, ClGBI was added at 200 and 800 μM final concentration for 2, 17, and 48 h before the different assays; for these experiments, in control condition, DMSO was added to a final concentration of 0.8% (equal to the 800 μM ClGBI wells) for 48 h.

Cell culture photographs

Ninety-six well plates were photographed with a Micrometrics CCD camera mounted on a Nikon Eclipse TS100 inverted microscope and analyzed with the Micrometrics SE Premium 4 software.

Flow cytometry pH_i determinations

The protocol described in Current Protocols in Cytometry (1997) [11] was used for pH measurement with BCECF using pseudo null calibration (also depicted by Franck et al. [17] and Eisner et al. [15], among others). Briefly, after incubation (see "In vitro exposure of Jurkat T cell line to Hv1 channel blockers for flow cytometry determinations" section), cells were centrifuged 5 min at 500 rpm and loaded with 2 μg/ml BCECF-AM 15 min at 37 °C, centrifuged, and resuspended in 10% FBS-HEPES solution. Prior to the measurement, every batch of cells was exposed to the corresponding blocker at the same concentration of incubation in order to prevent eventual pH_i recovery. Pseudo null calibration curve was performed according to Chow et al. [11] in each experiment (points pH = 8.0/7.7/7.4/7.1/6.8, see supplementary material Fig. S1). The fluorescence of BCECF was monitored by a FACSCalibur flow cytometer (Becton Dickinson) for an amount of 20,000 cells per tube. Data were acquired with CellQuest Pro 5.2.1 program and further analyzed with *Flowing Software v2.5.1* (by Perttu Terho, Turku Centre for Biotechnology, Finland) software. A two-order polynomial fitting between ratio of FL1/FL3 channels vs. calibration pH values was performed for each experiment (see supplementary material Fig. S1); the output equation was later used to calculate pH_i in each condition.

Flow cytometry annexin V binding determinations

In order to assess the extent of apoptosis after the incubation with Hv1 blockers (see "In vitro exposure of Jurkat T cell line to Hv1 channel blockers for flow cytometry determinations" section), annexin V binding was evaluated. In those experiments related with Zn^{2+}, annexin V-phycoerythrin (PE) labeling was performed, while in experiments regarding ClGBI, annexin V-FITC/propidium iodide (PI) double staining was employed [19].

After $ZnCl_2$ incubation, cells were stained with 1 μl commercial annexin V-PE in binding buffer (eBioscience) for each sample (average of 100,000 cells per well) in the dark for 15 min at room temperature. Later, cells were washed and resuspended in PBS solution. Fluorescence was detected using a FACSCalibur flow cytometer (Becton Dickinson) acquiring 20,000 cells per tube. Data were analyzed with FlowJo X 10.0.7 software.

In ClGBI incubation experiments, the same procedure was followed with the difference of using annexin V-FITC (instead of annexin V-PE) and a subsequent staining with 1 μg/ml PI 10 min in the dark (37 °C). Cells that were annexin V-$FITC^+$ (with translocation of phosphatidylserine from the inner to the outer leaflet of the plasma membrane) and PI^- (with intact cellular membrane) were considered as early apoptotic cells, whereas annexin V-$FITC^+$/PI^+ were considered late apoptotic/necrotic. For every independent experiment, the gates were assigned in order to distinguish heat treated (55 °C 20 min, double-positive controls) from fresh viable cells (double-negative control), as exemplified in supplementary material (Fig. S2).

Statistics

The results are expressed as mean ± standard error of the mean. Paired or unpaired Student's *t* tests were used to compare two groups. ANOVA (one-way or two-way, followed by Bonferroni post hoc test for means comparison) was used to compare three or more groups. In all cases, a *p* value lower than 0.05 was considered for establishing statistically significant differences. All statistics calculations have been done using OriginPro 9 software.

Reagents

BCECF-AM (Invitrogen Corporation, USA) and other flow cytometry reagents (annexin V-PE, annexin V-FITC, and propidium iodide) were purchased to Beckton and Dickinson (CA, USA). ClGBI (CAS no. 70590-32-8, PubChem CID 408159) was aquired from StruChem Co., Ltd. (Wujiang, China). All other reagents are from Sigma-Aldrich (St. Louis, MO) unless otherwise indicated. DMEM medium and FBS were purchased from local suppliers.

Results

Hv1 blockade by ClGBI

The presence of functional Hv1 channels in Jurkat T cells was reported by Schilling et al. [53] by patch clamp technique in the whole-cell configuration. They showed slow-activating H^+ currents evoked by membrane depolarization depending on transmembrane pH gradient and blocked by Zn^{2+}. In this work, we tested the presence of Hv1 currents in our Jurkat T cell batch confirming the functional presence of these channels with the same electrophysiological properties observed before [53] (see Supplementary Fig. S3).

Figure 1 shows the effect of a newly synthesized Hv1 inhibitor, ClGBI, on whole-cell currents mediated by Hv1 channels. ClGBI is a membrane-permeable compound reported recently by Dr. Tombola's group, which has demonstrated the inhibitory effect and the specific blocking mechanism of different guanidine-related compounds [24]. Figure 1 depicts that this Hv1 blocker inhibits the voltage-activated H^+ currents in leukemic Jurkat T cells, in a reversible and concentration-dependent manner. We tested 200, 500, and 800 μM ClGBI, observing a clear maximal drug effect from 500 μM.

Short-term pH_i regulation

We further analyze if the Hv1 channel inhibition, by Zn^{2+} or ClGBI, effectively produces Jurkat T cell acidification in the same temporal course that these blockers affect the H^+ currents. Considering previous reports showing the NHE exchanger as an important regulator of pH_i in this cell line [32], we firstly used Na^+-free extracellular solution to overcome its activity and isolate the potential effect of Hv1 inhibition on pH_i. In such condition, and using cuvette fluorometry with BCECF as intracellular pH indicator, we observed an immediate pH_i decrease when 1 mM

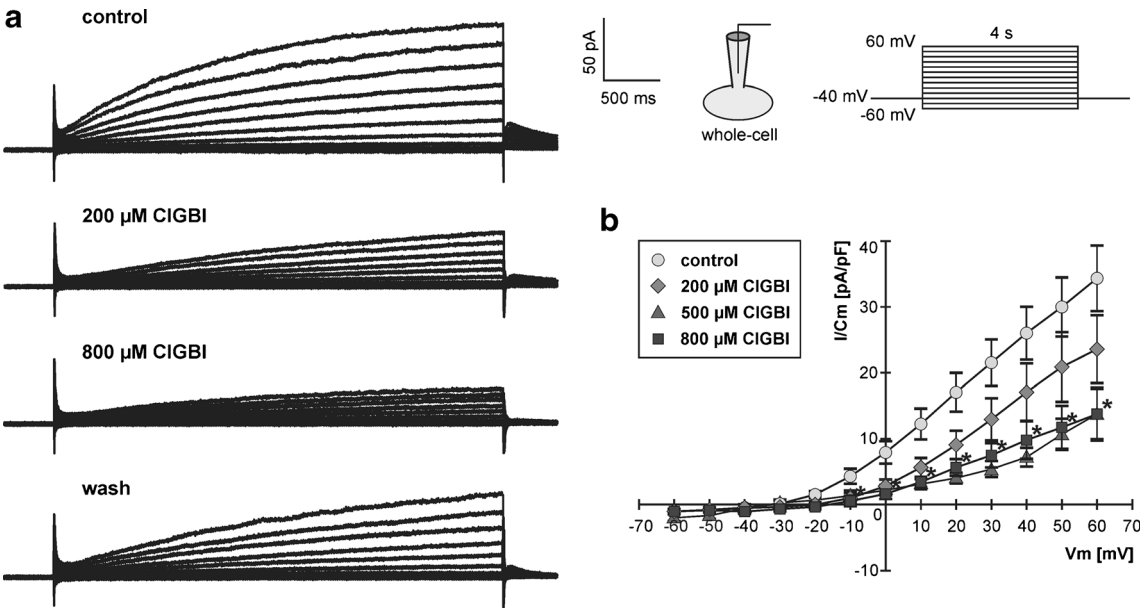

Fig. 1 ClGBI Hv1 current inhibition. **a** Superimposed representative whole-cell currents recorded in response to 4-s long pulses, stepping from a holding potential of −40 mV to levels ranging from +60 to −60 mV, with 10 mV increments in control conditions, after stable effect of different ClGBI concentrations and after the drug washout. **b** Mean ± SEM current density versus voltage (I-V) curves, corresponding to the control condition and ClGBI (200, 500, and 800 μM). The *asterisk* indicates a statistically significant difference by multiple comparison versus control group at each membrane potential ($n = 4–8$, $p < 0.05$)

Zn^{2+} or 200 μM ClGBI was added to the extracellular solution (Fig. 2a upper panel). Moreover, if we challenge the cells with an acidic stimulus such as a permeable propionic acid pulse, the pH_i recovery is significantly slower when Hv1 channels are inhibited, compared with the control condition (Fig. 2a, lower panel).

Furthermore, we tested the effect of ClGBI under physiological extracellular Na^+ concentration in order to see the impact of Hv1 blockade in the presence of active NHE (Fig. 2b, upper panel). According to the first result, even in the presence of such redundant mechanism, 200 μM ClGBI is able to affect basal pH_i inducing a significant acidification in 12 min and lowering the recovery rate after propionic acid pulse (Fig. 2b, lower panel). Although the differences in pH_i values obtained in both conditions (Hv1 inhibition with and without extracellular Na^+) indicate an important contribution of the NHE activity, the results clearly show a determinant role of the Hv1 channel in pH_i homeostasis.

Long-term pH_i regulation

We next evaluated the effect of long-term Hv1 inhibition on pH_i. Jurkat T cells were incubated with Zn^{2+} (1 mM, for 2 and 17 h) or ClGBI (200 and 800 μM, for 2, 17, and 48 h), and then, pH_i was measured by flow cytometry. In every case, time is considered as the number of hours where the cells were exposed to Hv1 inhibitors before cytometric measurements. Figure 3 (left panels) shows the obtained results expressed as mean values of total cells for each condition. These figures clearly show that in both cases, Hv1 inhibition induced by Zn^{2+} (Fig. 3a) or by the more selective Hv1 blocker ClGBI (Fig. 3b) produces a significant time-dependent long-lasting acidification in Jurkat T cells. The effect of ClGBI was also dependent on drug concentration. Cumulative % of acidified cells illustrates (Fig. 3a, b, right panels) the progression of acidification as the amount of total cells whose pH_i falls below defined cutoff values (7.0, 6.9, and 6.8). Strong Hv1 blockade (1 mM Zn^{2+} and 800 μM ClGBI) derives in a vast majority of cells with pH_i below 7.0 in 2 h, whereas values at 48 h show that these cells continued acidification below 6.8. In the lower blockade condition (200 μM ClGBI), longer periods of time are required to reach a significant percentage of cells to fall below the same acid cutoff values.

Abnormal growing pattern

Moreover, we observed that the typical growing pattern of Jurkat T cells (first line Fig. 4) was visibly affected by Hv1 blocker incubation. Figure 4 shows 100× photographs of the time course of cell culture in control conditions (presence of DMSO 0.8%) and 200 and 800 μM of ClGBI. The presence of the Hv1 blocker avoids clump formation, a natural feature of proper growing. The same effect was observed with Zn^{2+} (data not shown). Although these observations are not precise about the involved mechanisms in the abnormal growing pattern, the presence of augmented cell death or proliferation arrest is evident which could be the consequence of acidification produced by Hv1 inhibition.

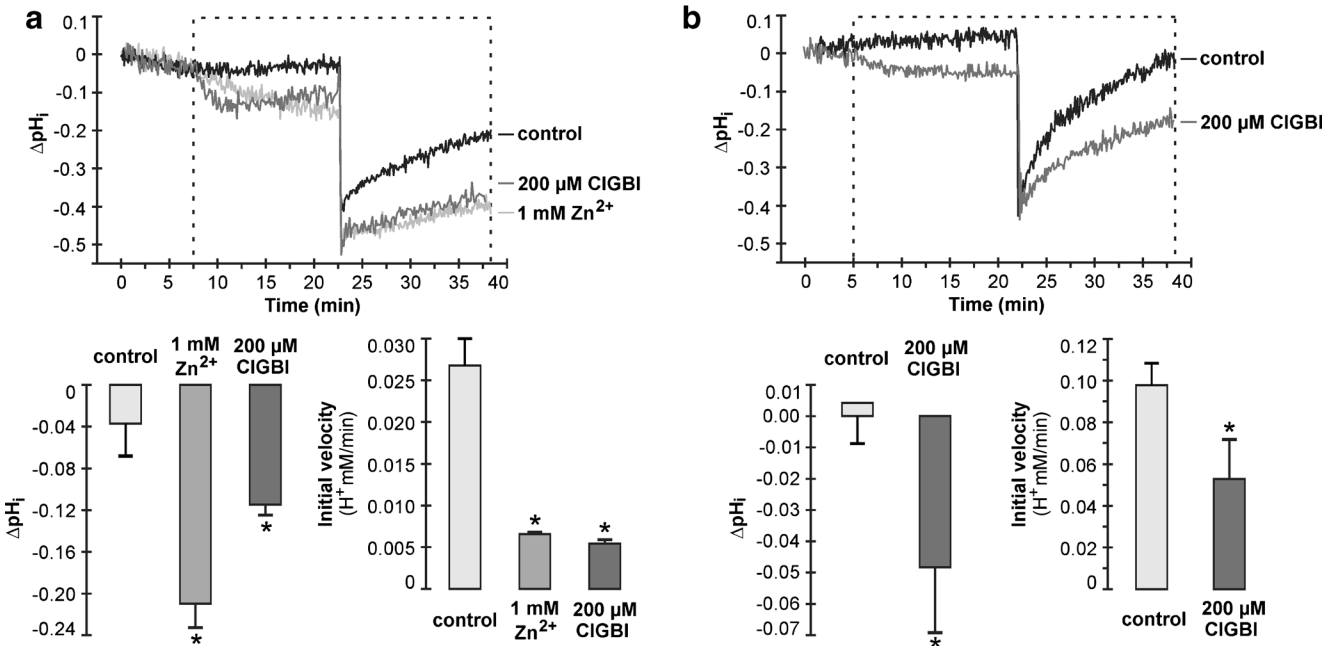

Fig. 2 Intracellular pH regulation in Jurkat T cells. Representative experiments of pH_i changes after blockade of Hv1 channel with 1 mM Zn^{2+} or 200 μM ClGBI (*dotted line boxes*) in free sodium HEPES-buffered solution (avoiding NHE activity, **a**) or in the presence of sodium (**b**). In the two cases, basal pH_i decreases when the Hv1 was blocked (average in **a** and **b**). After 20 min, in both experiments, Jurkat T cells were acidified with propionic acid and initial rates of pH_i recovery were estimated from the slope of the line fitted by the least squares method. *Asterisk* indicates statistically significant differences by one-way ANOVA (**a**, $n = 6$) and Student's t test (**b**, $n = 6$), $p < 0.05$

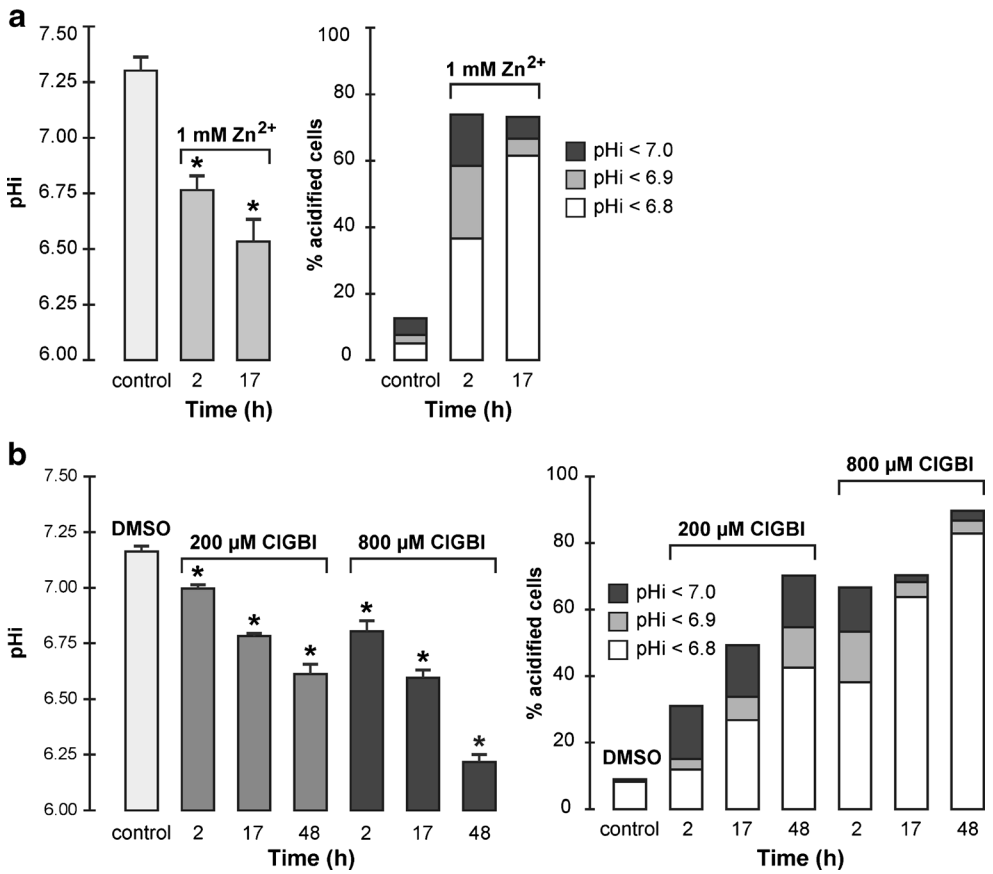

Fig. 3 Long-term pH_i determinations. **a** Mean values of pH_i in control condition (DMEM medium 17 h) and after 2 and 17 h of 1 mM Zn^{2+} exposure in culture conditions (*left panel*). The *asterisks* indicate statistically significant differences by one-way ANOVA test ($n = 4$, $p < 0.05$). Time course of percentage of the total cells with pH_i values below 7.0, 6.9, and 6.8 in Zn^{2+} treatment (*right panel*). **b** Mean values of pH_i in control condition and after 2, 17, and 48 h of 200 and 800 μM ClGBI exposure in culture conditions (*left panel*). The *asterisk* means statistically significant effects by two-way ANOVA ($n = 4$, $p < 0.05$). Time course of percentage of the total cells with pH_i values below 7.0, 6.9, and 6.8 exposed to 200 or 800 μM ClGBI (*right panel*). Controls are in both cases, and vehicles applied at the higher concentration and longer period of treatment (DMSO 0.8% for 48 h)

Cell acidification is associated with apoptosis-mediated cell death

Therefore, we specifically evaluated by flow cytometry if Hv1 inhibition is able to induce Jurkat T cell apoptosis measuring breakdown of phosphatidylserine asymmetry of the plasma membrane using fluorochrome-labeled annexin V [19] and plasma membrane status with PI. Figure 5 show the corresponding plots for the different conditions and the mean values obtained with blockers. We could observe that 2 h after the addition of 1 mM Zn^{2+}, a significant increase (20.2 ± 3.7%) in the frequency of annexin V^+ cells was produced over the percentage of control condition, whereas in overnight exposure (17 h), this difference ascended to 47.8 ± 7.0%, indicating that Zn^{2+} acidification is followed by apoptosis induction sharing both processes a common time course. Interestingly, ClGBI also produces apoptosis and finally cell death, in a time-dependent manner, according to the pH results. The concentration effect is significant in late apoptotic (annexin V-$FITC^+$/PI^+) and viable (annexin V-$FITC^-$/PI^-) cells but not in early apoptotic (annexin V-$FITC^+$/PI^-) population (two-way ANOVA $p > 0.05$, $n = 4$–7). This latter result suggests that higher amounts of ClGBI (hence a more pronounced acidification) exert apoptosis induction in the same rate than 200 μM. However, this should be taken with caution considering that at 2 h, there seems to be a difference in early apoptotic cells between the two concentrations (not statistically significant), and particularly at 800 μM, this population declines over time at expenses of late apoptotic cell increase, while at 200 μM, percentage of annexin V-$FITC^+$/PI^- is raising up to 48 h as the double-positive population develops a lower increase. This interpretation may be more in accordance with a statistically significant effect of dose over % of viable cells.

Discussion

A new role of Hv1 channels in Jurkat T cells is set forth in this work. For the first time, we present detailed evidence showing

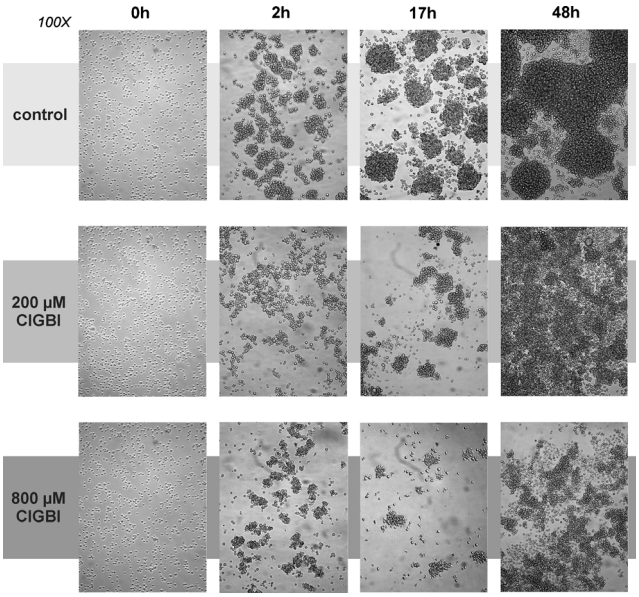

Fig. 4 Jurkat T cells' growing pattern. Photographs taken at different times after 0.8% DMSO (ClGBI solvent), 200 and 800 μM ClGBI addition to the culture media. Note the difference in clump formation in the three conditions. Superior views of culture petri dishes, ×100 magnification

that both two Hv1 channel inhibitors induce intracellular acidification in the same temporal course, as measured current blockade, and how this pH_i decay is intensified under long-term culture conditions in a dose-dependent and time-dependent manner, being this paralleled by apoptosis induction monitored with annexin V-PI staining, giving new evidences of cell death routines involved. Although acidification is a known and relevant factor involved in apoptosis, our work highlights the point that Hv1 channel inhibition is enough to produce an increasing frequency of dead cells through apoptosis (Fig. 6)..

In the last 10 years, the knowledge of biophysical properties of Hv1 channels has increased notably, mainly obtained in heterologous expression systems as *Xenopus* oocytes, which are very useful to study in deep Hv1 kinetic, conductance, voltage, and pH dependence among other properties [13, 20, 47]. However, the physiological and pharmacological regulation of these channels is mostly unknown yet. In our work, we show that the newly synthesized compound ClGBI blocks Hv1 channel in Jurkat T cells as Zn^{2+} do. Although Zn^{2+} has been extensively used to block the heterologous expressed Hv1 channel, in a native system, the results could be confusing due to its diverse known cellular effects [10, 25, 26, 61]. Here, we show that a more selective blocker, ClGBI, is a new useful pharmacological tool to test the functional role of these channels in native cells. Considering that it is a novel compound, we cannot discard additional effects that might influence the final effects of this drug; nevertheless, both blockers derived in the same results above strengthening the idea of Hv1 involvement.

Using ClGBI to induce Hv1 inhibition, we demonstrated a tight link between Hv1 channel activity and pH_i regulation in Jurkat T cells. While short-term Hv1 blockade induces a little but significant baseline pH_i decrement, long-term inhibition points out a requirement of Hv1 activity for pH_i homeostasis. Together, these results indicate that in these leukemic cells, this structure is useful not only for rapid recovery after acid loads but also for basal proton extrusion. In cancer cells, the current knowledge indicates that neoplastic transformation is associated with a metabolic deregulation which induces a significant acid overproduction, commonly known as the Warburg effect [29, 56]. Thus, the role of this ion channel consuming the pH gradient to extrude H^+ without metabolic energetic cost represents a novel counterbalance mechanism, mostly ignored compared with the well-characterized H^+ active transporters described to prevent cancer cell acidification. Namely, the NHE, proton pump V-ATPase, bicarbonate (HCO_3^-) transporter, and proton-lactate symporter require a direct or indirect expend of metabolic energy to perform its function [12, 58]. In addition, Hv1 conductivity is also strongly regulated by pH across the membrane, as the activation $V_{1/2}$ values raise markedly when extracellular pH decreases [13], making the channel opening only possible for H^+ extrusion. Thus, this salient feature makes Hv1 function as a perfect proton valve, preventing an eventual H^+ entry under acidic media like solid tumors or inflammatory environment (as one might speculate considering that Hv1 is a passive transport pathway).

Furthermore, in this work, we show that Hv1 inhibition, with Zn^{2+} or ClGBI, not only produces a significant acidification of Jurkat T cells but also induces apoptosis and finally cell death. After 2 h of Hv1 inhibition, the apoptotic process starts and progresses to about 45% of cell death after 48 h of Hv1 inhibition with the maximal ClGBI concentration. In the same conditions (ClGBI during 48 h), the pH_i of these cells progresses from a normal pH_i to values below 6.8. Although a few studies showed an early apoptosis-related intracellular alkalinization [3, 28], acidification is widely reported in both apoptosis pathways, "mitochondria-dependent" (intrinsic) or "death receptor" (extrinsic) (for a detailed revision, see Lagadic-Gossmann and Lecureur [31] and Matsuyama and Reed [38]). In the extrinsic pathway acidification, it has been described a downstream caspase activation preceding mitochondrial dysfunction [35], while in the intrinsic one, acidification appears to be caspase-independent and previous to this protease activation [37]. In Jurkat T cells, Gottlieb et al. described intracellular acidification in both pathway-related stimuli and showed how intracellular alkalinization reverted apoptosis progression [22]. Moreover, Jurkat T cell apoptosis has been described, prior to our work, to be induced by cellular acidification due to NHE1 inhibition [50]. According to these events, caspases [18, 37, 51, 54], endonucleases [2, 16], and some of the Bcl-2 family proteins [30, 59] have been

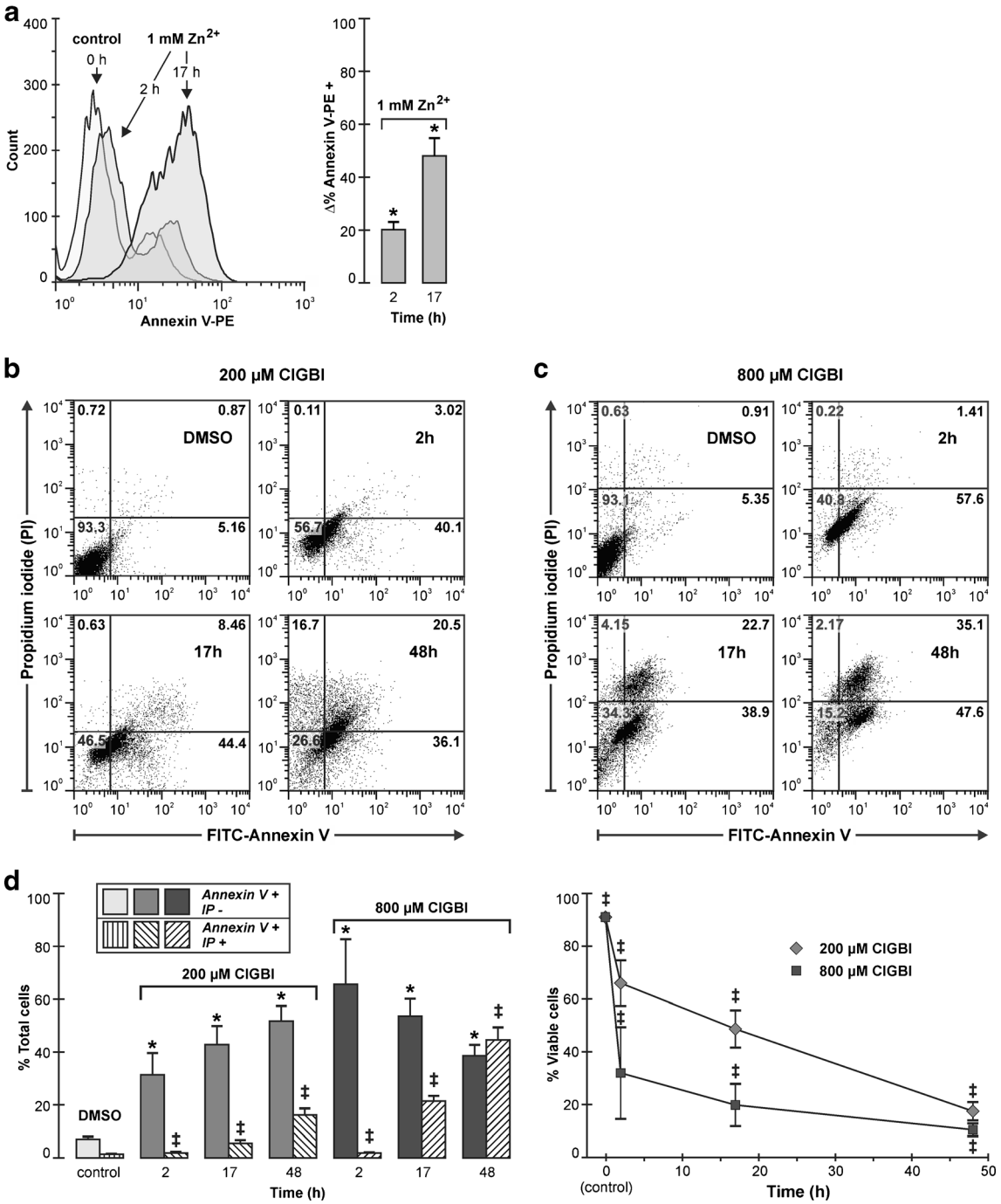

Fig. 5 Hv1 blockade is associated with apoptosis-mediated cell death. **a** Representative histograms of annexin V-PE labeling intensity of 1 mM Zn^{+2}-treated cells: 2 and 17 h and control conditions (*left panel*). Mean values ± SEM of the difference between each condition and its own control in % of annexin V-PE-positive cells (*right panel*). The *asterisk* means statistically significant difference from zero and between each other ($p < 0.05$, Student's *t* test, $n = 4$). **b** Representative dot plots of annexin V-FITC vs PI for different times of 200 μM ClGBI treatment. **c** Equivalent figure for 800 μM ClGBI treatment. **d** Mean % values ± SEM for early apoptotic (annexin V-FITC$^+$/PI$^-$) and late apoptotic/necrotic (annexin V-FITC$^+$/PI$^+$) cell populations at different times of ClGBI incubation (*left panel*). Decrement in % of viable cells (annexin V-FITC$^-$/PI$^-$) along ClGBI incubation (*right panel*). The *double daggers* indicate that viable and late apoptotic populations are affected significantly by incubation time and ClGBI concentration. The *asterisk* means that early apoptotic cells are significantly affected by time but not by ClGBI concentration (two-way ANOVA, $p < 0.05$, $n = 4$–7)

shown as pH_i-sensitive structures clearly responsible for apoptosis execution. Therefore, in this tight link between leukemic cell death and pH_i regulation, the Hv1 channel emerges as a new interesting structure.

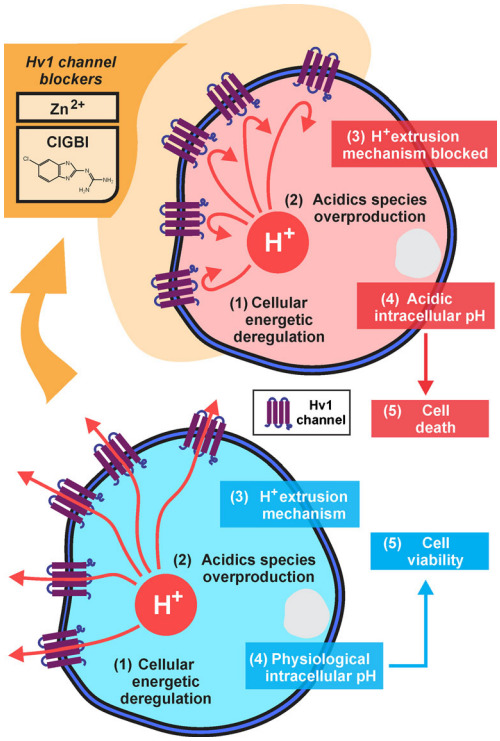

Fig. 6 The inhibition of voltage-gated H^+ channel induces intracellular acidification promoting cell death by apoptosis in the cell line studied. Depiction representing the hypothesis of Hv1 channel role in the context of neoplastic cells: Jurkat T lymphocytes, as other neoplastic cells, obtain energy via glycolytic pathways producing a high amount of acidic species that must be removed to the extracellular milieu. Blocking H^+ extrusion structures, mainly Hv1 channel, produces intracellular acidification that further derives in apoptosis

Ion channels are also frequently implicated in the control of proliferation, apoptosis, and cell migration of cancer cells, and the leukemic cells are not the exception. Recently, Arcangeli et al. reviewed the experimental and preclinical evidence that have ion channels as biological target in leukemia treatment [1]. However, up to date, no review of the field has mentioned Hv1 as a channel to be considered in apoptosis. In the same line, another feature to be further evaluated is if Hv1 blockade derives in membrane depolarization, another event coherent with apoptosis development [4, 43]. The use of new drugs or endogenous modulators that could selectively inhibit the channel may be useful not only in leukemia cells but also in solid tumors; recent works have shown that Hv1 downregulation or inhibition decreases the migratory and invasive abilities of highly metastatic colorectal [64], human breast [62, 63], and glioma [65] tumor cell, as well as impairing proliferation. Latest reports from the field reveal that Hv1 is also functionally expressed in human glioblastoma multiforme cells to which Zn^{2+} treatment induces cell death (PI staining), notwithstanding that significant intracellular acidification is only seen under extracellular Na^+ deprivation [49].

Our work presents evidences suggesting that Hv1 inhibition might be a new and promising therapeutic target in leukemia treatment. It is worthwhile to note that KO mice lacking Hv1 channel are not associated with immunosuppression [48, 52], although decreased ROS production. Indeed, Clapham et al. challenged $Hv1^{-/-}$ mice against *Staphylococcus aureus* intraperitoneal injection, *Pseudomonas aeurginosa*, and *Burkholderia cepacia* nasal inoculation and were unable to see a significant impairment on bacterial clearance in vivo compared with *w/w* mice [48]. These facts let us speculate that Hv1 pharmacological inhibition might be a safe strategy in oncohematological diseases in contrast to classical antineoplastic drugs. This work, among others, may contribute to keeping this potent structure in mind.

Acknowledgements The authors wish to thank Mr. Angel Flores, Ms. Julia De Santis, and Mr. Leandro Diaz Zegarra for their technical assistance. This study was financially supported by grant 11X652 Universidad Nacional de La Plata to Verónica Milesi, Fondecyt grant 1160261 to Carlos González León, PICT 2014-0603 to Pedro Martín, and PICT 2012-1772 to Guillermo Docena from the Agencia Nacional de Promoción Científica y Tecnológica (ANPCYT).

Compliance with ethical standards

Conflict of interest The authors declare that they have no conflict of interest.

References

1. Arcangeli A, Pillozzi S, Becchetti A (2012) Targeting ion channels in Leukemias: a new challenge for treatment. Curr Med Chem 19: 683–696
2. Barry MA, Eastman A (1993) Identification of deoxyribonuclease II as an endonuclease involved in apoptosis. Arch Biochem Biophys 300:440–450. doi:10.1006/abbi.1993.1060
3. Belaud-Rotureau MA, Leducq N, De Gannes FMP, Diolez P, Lacoste L, Lacombe F, Bernard P, Belloc F (2000) Early transitory rise in intracellular pH leads to Bax conformation change during ceramide-induced apoptosis. Apoptosis 5:551–560. doi:10.1023/A:1009693630664
4. Bortner CD, Gómez-Angelats M, Cidlowski JA (2001) Plasma membrane depolarization without repolarization is an early molecular event in anti-Fas-induced apoptosis. J Biol Chem 276:4304–4314. doi:10.1074/jbc.M005171200
5. Byerly LOU, Meech R, Moody WJ (1984) Rapidly activating hydrogen ion currents in perfused neurones of the snail, *LYMNAEA STAGNALIS*. J Physiol 351:199–216
6. Capasso M, Bhamrah MK, Henley T, Boyd RS, Langlais C, Cain K, Dinsdale D, Pulford K, Khan M, Musset B, Cherny VV, Morgan D, Gascoyne RD, Vigorito E, DeCoursey TE, MacLennan ICM, Dyer MJS (2010) HVCN1 modulates BCR signal strength via regulation of BCR-dependent generation of reactive oxygen species. Nat Immunol 11:265–272. doi:10.1038/ni.1843
7. El Chemaly A, Guinamard R, Demion M, Fares N, Jebara V, Faivre JF, Bois P (2006) A voltage-activated proton current in human cardiac fibroblasts. Biochem Biophys Res Commun 340:512–516. doi:10.1016/j.bbrc.2005.12.038

8. El Chemaly A, Okochi Y, Sasaki M, Arnaudeau S, Okamura Y, Demaurex N (2010) VSOP/Hv1 proton channels sustain calcium entry, neutrophil migration, and superoxide production by limiting cell depolarization and acidification. J Exp Med 207:129–139. doi:10.1084/jem.20091837
9. Cherny VV, Murphy R, Sokolov V, Levis RA, Decoursey TE (2003) Properties of single voltage-gated proton channels in human eosinophils estimated by noise analysis and by direct measurement. J Gen Physiol. doi:10.1085/jgp.200308813
10. Chimienti F, Seve M, Richard S, Mathieu J, Favier A (2001) Role of cellular zinc in programmed cell death: temporal relationship between zinc depletion, activation of caspases, and cleavage of Sp family transcription factors. Biochem Pharmacol 62:51–62. doi:10.1016/S0006-2952(01)00624-4
11. Chow S, Hedley D (1997) Flow cytometric measurement of intracellular pH. Curr Protoc Cytom 9
12. Counillon L, Bouret Y, Marchiq I, Pouysségur J (2016) Na+/H+ antiporter (NHE1) and lactate/H+ symporters (MCTs) in pH homeostasis and cancer metabolism. BBA - Mol Cell Res. doi:10.1016/j.bbamcr.2016.02.018
13. DeCoursey TE (2008) Voltage-gated proton channels. Cell Mol Life Sci 65:2554–2573. doi:10.1007/s00018-008-8056-8
14. DeCoursey TE, Cherny VV (1993) Potential, pH, and arachidonate gate hydrogen ion currents in human neutrophils. Biophys J 65: 1590–1598. doi:10.1016/S0006-3495(93)81198-6
15. Eisner DA, Kenning NA, Neill SCO, Pocock G, Richards CD, Valdeolmillos M (1989) A novel method for absolute calibration of intracellular pH indicators. Pflugers. Arch Eur J Physiol 413: 553–558. doi:10.1007/BF00594188
16. Famulski KS, Macdonald D, Paterson MC, Sikora E (1999) Activation of a low pH-dependent nuclease by apoptotic agents. Cell Death Differ 6:281–289. doi:10.1038/sj.cdd.4400495
17. Franck P (1996) Measurement of intracellular pH in cultured cells by flow cytometry with BCECF-AM. J Biotechnol 46:187–195. doi:10.1016/0168-1656(95)00189-1
18. Furlong IJ, Ascaso R, Lopez Rivas A, Collins MK (1997) Intracellular acidification induces apoptosis by stimulating ICE-like protease activity. J Cell Sci 110:653–661
19. Koopman G, Reutelingsperger CPM, Kuijten GAM, Keehnen RMJ, Pals ST, van MHJ O (1994) Annexin V for flow cytometric detection of phosphatidylserine expression on B cells undergoing apoptosis. Blood 84:1415–1420
20. Gonzalez C, Rebolledo S, Perez ME, Larsson HP (2013) Molecular mechanism of voltage sensing in voltage-gated proton channels. J Gen Physiol 141:275–285. doi:10.1085/jgp.201210857
21. Gordienko DV, Tare M, Parveen S, Fenech CJ, Robinson C, Bolton TB (1996) Voltage-activated proton current in eosinophils from human blood. J Physiol 496:299–316. doi:10.1113/jphysiol.1996.sp021686
22. Gottlieb R a, Nordberg J, Skowronski E, Babior BM (1996) Apoptosis induced in Jurkat cells by several agents is preceded by intracellular acidification. Proc Natl Acad Sci U S A 93:654–658. doi:10.1073/pnas.93.2.654
23. Hamill OP, Marty A, Neher E, Sakmann B, Sigworth FJ (1981) Improved patch-clamp techniques for high-resolution current recording from cells and cell-free membrane patches. Pflugers Arch Eur J Physiol. Arch Eur J Physiol 391:85–100. doi:10.1007/BF00656997
24. Hong L, Kim IH, Tombola F (2014) Molecular determinants of Hv1 proton channel inhibition by guanidine derivatives. Proc Natl Acad Sci U S A 111:9971–9976. doi:10.1073/pnas.1324012111
25. Huber KL, Hardy JA (2012) Mechanism of zinc-mediated inhibition of caspase-9. Protein Sci 21:1056–1065. doi:10.1002/pro.2090
26. Jiménez Del Río M, Vélez-Pardo C (2004) Transition metal-induced apoptosis in lymphocytes via hydroxyl radical generation, mitochondria dysfunction, and caspase-3 activation: an in vitro model for neurodegeneration. Arch Med Res 35:185–193. doi:10.1016/j.arcmed.2004.01.001
27. Kapus A, Romanek R, Grinstein S (1994) Arachidonic acid stimulates the plasma membrane H+ conductance of macrophages. J Biol Chem 269:4736–4745
28. Kim J, Bae HAER, Park BS, Lee JEM, Ahn HEEB, Rho JHEEH, Yoo KW, Park WOOC, Rho SHAEH, Yoon HEES, Yoo YH (2003) Early mitochondrial hyperpolarization and intracellular alkalinization in lactacystin-induced apoptosis of retinal pigment epithelial cells. J Pharmacol Exp Ther 305:474–481. doi:10.1124/jpet.102.047811
29. Kim JW, Dang CV (2006) Cancer's molecular sweet tooth and the Warburg effect. Cancer Res 66:8927–8930. doi:10.1158/0008-5472.CAN-06-1501
30. Kubasiak LA, Hernandez OM, Bishopric NH, Webster KA (2002) Hypoxia and acidosis activate cardiac myocyte death through the Bcl-2 family protein BNIP3. Proc Natl Acad Sci U S A 99:12825–12830. doi:10.1073/pnas.202474099
31. Lagadic-Gossmann D, Huc L, Lecureur V (2004) Alterations of intracellular pH homeostasis in apoptosis: origins and roles. Cell Death Differ 11:953–961. doi:10.1038/sj.cdd.4401466
32. Lang F, Madlung J, Bock J, Lükewille U, Kaltenbach S, Lang KS, Belka C, Wagner CA, Lang HJ, Gulbins E, Lepple-Wienhues A (2000) Inhibition of Jurkat-T-lymphocyte Na+/H+-exchanger by CD95(Fas/Apo-1)-receptor stimulation. Pflügers Arch - Eur J Physiol 440:902–907. doi:10.1007/s004240000358
33. Levine AP, Duchen MR, De Villiers S, Rich PR, Segal AW (2015) Alkalinity of neutrophil phagocytic vacuoles is modulated by HVCN1 and has consequences for myeloperoxidase activity. PLoS One 10:1–20. doi:10.1371/journal.pone.0125906
34. Lishko PV, Botchkina IL, Fedorenko A, Kirichok Y (2010) Acid extrusion from human spermatozoa is mediated by flagellar voltage-gated proton channel. Cell 140:327–337. doi:10.1016/j.cell.2009.12.053
35. Liu D, Martino G, Thangaraju M, Sharma M, Halwani F, Shen SH, Patel YC, Srikant CB (2000) Caspase-8-mediated intracellular acidification precedes mitochondrial dysfunction in somatostatin-induced apoptosis. J Biol Chem 275:9244–9250. doi:10.1074/jbc.275.13.9244
36. Marches R, Vitetta ES, Uhr JW (2001) A role for intracellular pH in membrane IgM-mediated cell death of human B lymphomas. Proc Natl Acad Sci U S A 98:3434–3439. doi:10.1073/pnas.061028998
37. Matsuyama S, Llopis J, Deveraux QL, Tsien RY, Reed JC (2000) Changes in intramitochondrial and cytosolic pH: early events that modulate caspase activation during apoptosis. Nat Cell Biol 2:318–325. doi:10.1038/35014006
38. Matsuyama S, Reed JC (2000) Mitochondria-dependent apoptosis and cellular pH regulation. Cell Death Differ 7:1155–1165. doi:10.1038/sj.cdd.4400779
39. Morgan D, Cherny VV, Finnegan A, Bollinger J, Gelb MH, DeCoursey TE (2007) Sustained activation of proton channels and NADPH oxidase in human eosinophils and murine granulocytes requires PKC but not cPLA2 alpha activity. J Physiol 579:327–344. doi:10.1113/jphysiol.2006.124248
40. Murphy R, Cherny VV, Morgan D, DeCoursey TE (2005) Voltage-gated proton channels help regulate pHi in rat alveolar epithelium. Am J Physiol Lung Cell Mol Physiol 288:L398–L408. doi:10.1152/ajplung.00299.2004
41. Musset B, Decoursey T (2012) Biophysical properties of the voltage-gated proton channel HV1. Wiley Interdiscip Rev Membr Transp Signal 1:605–620. doi:10.1002/wmts.55
42. Musset B, Smith SME, Rajan S, Morgan D, Cherny VV, DeCoursey TE (2011) Aspartate 112 is the selectivity filter of the human voltage-gated proton channel. Nature 480:273–277. doi:10.1038/nature10557

43. Nolte F, Friedrich O, Rojewski M, Fink RH a, Schrezenmeier H, Körper S (2004) Depolarisation of the plasma membrane in the arsenic trioxide (As2O3)-and anti-CD95-induced apoptosis in myeloid cells. FEBS Lett 578:85–89. doi:10.1016/j.febslet.2004.10.075
44. Nordström T, Rotstein OD, Romanek R, Asotra S, Heersche JNM, Manolson MF, Brisseau GF, Grinstein S (1995) Regulation of cytoplasmic pH in osteoclasts: contribution of proton pumps and a proton-selective conductance. J Biol Chem 270:2203–2212. doi:10.1074/jbc.270.5.2203
45. Ollig J, Kloubert V, Weßels I, Haase H, Rink L (2016) Parameters influencing zinc in experimental systems in vivo and in vitro. Metals (Basel) 6(71). doi:10.3390/met6030071
46. Petheo GL, Orient A, Baráth M, Kovács I, Réthi B, Lányi Á, Rajki A, Rajnavölgyi É, Geiszt M (2010) Molecular and functional characterization of Hv1 proton channel in human granulocytes. PLoS One. doi:10.1371/journal.pone.0014081
47. Qiu F, Rebolledo S, Gonzalez C, Larsson HP (2013) Subunit interactions during cooperative opening of voltage-gated proton channels. Neuron 77:288–298. doi:10.1016/j.neuron.2012.12.021
48. Ramsey IS, Ruchti E, Kaczmarek JS, Clapham DE (2009) Hv1 proton channels are required for high-level NADPH oxidase-dependent superoxide production during the phagocyte respiratory burst. Proc Natl Acad Sci U S A 106:7642–7647. doi:10.1073/pnas.0902761106
49. Ribeiro-Silva L, Queiroz FO, da Silva AMB, Hirata AE, Arcisio-Miranda M (2016) Voltage-gated proton channels in human glioblastoma multiforme cells. ACS Chem Neurosci acschemneuro 6b00083. doi:10.1021/acschemneuro.6b00083
50. Rich IN, Worthington-White D, Garden O a, Musk P (2000) Apoptosis of leukemic cells accompanies reduction in intracellular pH after targeted inhibition of the Na(+)/H(+) exchanger. Blood 95:1427–1434
51. Roy S, Bayly CI, Gareau Y, Houtzager VM, Kargman S, Keen SL, Rowland K, Seiden IM, Thornberry N a, Nicholson DW (2001) Maintenance of caspase-3 proenzyme dormancy by an intrinsic "safety catch" regulatory tripeptide. Proc Natl Acad Sci U S A 98:6132–6137. doi:10.1073/pnas.111085198
52. Sasaki M, Tojo A, Okochi Y, Miyawaki N, Kamimura D, Yamaguchi A, Murakami M, Okamura Y (2013) Autoimmune disorder phenotypes in Hvcn1-deficient mice. Biochem J 450:295–301. doi:10.1042/BJ20121188
53. Schilling T, Gratopp A, DeCoursey TE, Eder C (2002) Voltage-activated proton currents in human lymphocytes. J Physiol 545:93–105. doi:10.1113/jphysiol.2002.028878
54. Segal MS, Beem E (2001) Effect of pH, ionic charge, and osmolality on cytochrome c-mediated caspase-3 activity. Am J Physiol Cell Physiol 281:C1196–C1204
55. Seredenina T, Demaurex N, Krause K (2014) Voltage-gated proton channels as novel drug targets: from NADPH oxidase regulation to sperm biology. Antioxid Redox Signal 0:1–63. doi:10.1089/ars.2013.5806
56. Shanmugam M, McBrayer SK, Rosen ST (2009) Targeting the Warburg effect in hematological malignancies: from PET to therapy. Curr Opin Oncol 21:531–536. doi:10.1097/CCO.0b013e32832f57ec
57. Simchowitz L, Cragoe EJ Jr (1987) Intracellular acidification-induced alkali metal cation/H+ exchange in human neutrophils. JGenPhysiol 90:737–762. doi:10.1085/jgp.90.5.737
58. Spugnini EP, Sonveaux P, Stock C, Perez-Sayans M, De Milito A, Avnet S, Garcìa AG, Harguindey S, Fais S (2015) Proton channels and exchangers in cancer. Biochim Biophys Acta - Biomembr 1848:2715–2726. doi:10.1016/j.bbamem.2014.10.015
59. Tafani M, Cohn JA, Karpinich NO, Rothman RJ, Russo MA, Farber JL (2002) Regulation of intracellular pH mediates Bax activation in HeLa cells treated with staurosporine or tumor necrosis factor-α. J Biol Chem 277:49569–49576. doi:10.1074/jbc.M208915200
60. Thomas RC, Meech RW (1982) Hydrogen ion currents and intracellular pH in depolarized voltage-clamped snail neurones. Nature 299:826–828. doi:10.1038/299826a0
61. Velázquez-Delgado EM, Hardy JA (2012) Zinc-mediated allosteric inhibition of caspase-6. J Biol Chem 287:36000–36011. doi:10.1074/jbc.M112.397752
62. Wang Y, Li SJ, Pan J, Che Y, Yin J, Zhao Q (2011) Specific expression of the human voltage-gated proton channel Hv1 in highly metastatic breast cancer cells, promotes tumor progression and metastasis. Biochem Biophys Res Commun 412:353–359. doi:10.1016/j.bbrc.2011.07.102
63. Wang Y, Li SJ, Wu X, Che Y, Li Q (2012) Clinicopathological and biological significance of human voltage-gated proton channel Hv1 protein overexpression in breast cancer. J Biol Chem 287:13877–13888. doi:10.1074/jbc.M112.345280
64. Wang Y, Wu X, Li Q, Zhang S, Li SJ (2013) Human voltage-gated proton channel Hv1: a new potential biomarker for diagnosis and prognosis of colorectal cancer. PLoS One. doi:10.1371/journal.pone.0070550
65. Wang Y, Zhang S, Li SJ (2013) Zn2+ induces apoptosis in human highly metastatic SHG-44 glioma cells, through inhibiting activity of the voltage-gated proton channel Hv1. Biochem Biophys Res Commun 438:312–317. doi:10.1016/j.bbrc.2013.07.067